

SUPPLEMENTARY INFORMATION:

Glycophagy is an ancient bilaterian pathway supporting metabolic adaptation through STBD1 structural evolution

Liting Ren,^{1,4} Yitian Bai,^{1,4} Chenyu Shi,¹ Qi Li,^{1,2} Daniel J Macqueen,³ Shikai Liu,^{1,2,*}

¹Key Laboratory of Mariculture (Ocean University of China), Ministry of Education, and College of Fisheries, Ocean University of China, Qingdao 266003, China.

²Laboratory for Marine Fisheries Science and Food Production Processes, Qingdao Marine Science and Technology Center, Qingdao, Shandong 266237, China.

³The Roslin Institute and Royal (Dick) School of Veterinary Studies, The University of Edinburgh, Midlothian, United Kingdom.

⁴These authors contributed equally: Liting Ren, Yitian Bai.

*e-mail: liushk@ouc.edu.cn

Supplemental information list:

This PDF file includes:

Figures S1 to S7

Other supporting information for this manuscript include the following:

Tables S1 and S2 (provided as a separate Excel file)

Data S1-S3 (provided as a separate Excel file)

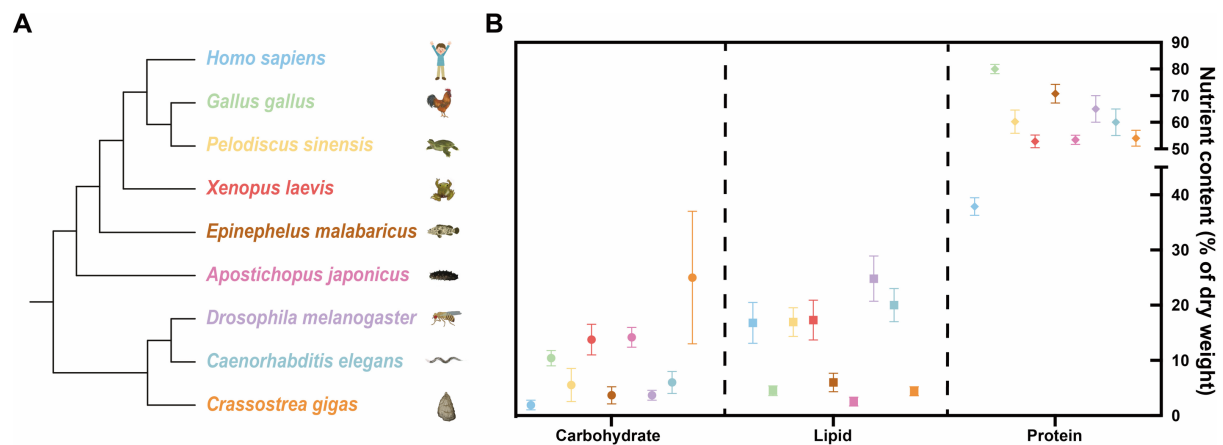


Fig. S1. Carbohydrate, lipid and protein storage across the Metazoa. **A** Phylogenetic tree for representative species. **B** Dry weight composition of carbohydrates, lipids, and proteins in *Homo sapiens* (adult man) was $1.91 \pm 0.87\%$, $16.8 \pm 3.7\%$, and $37.88 \pm 1.6\%^{1-3}$; *Gallus gallus* was $10.4 \pm 1.39\%$, $4.50 \pm 0.57\%$, and $79.98 \pm 1.69\%^{4}$; *Pelodiscus sinensis* was $5.52 \pm 3\%$, $16.94 \pm 2.6\%$, and $60.22 \pm 4.37\%^{5}$; *Xenopus laevis* (male) was $13.7 \pm 2.77\%$, $17.3 \pm 3.6\%$, and $52.8 \pm 2.4\%^{6}$; *Epinephelus malabaricus* was $3.67 \pm 1.55\%$, $6.00 \pm 1.67\%$, and $70.74 \pm 2.52\%^{7}$; *Apostichopus japonicus* was $14.17 \pm 1.79\%$, $2.54 \pm 0.21\%$, and $53.42 \pm 1.22\%^{8}$; *Drosophila melanogaster* was $3.69 \pm 0.9\%$, $24.8 \pm 4.1\%$, and $65 \pm 5\%^{9,10}$; *Caenorhabditis elegans* was $6 \pm 2\%$, $20 \pm 3\%$, and $60 \pm 5\%^{11}$, and *Crassostrea gigas* was $25 \pm 12\%$, $4.4 \pm 0.8\%$, and $54 \pm 3\%^{12}$.

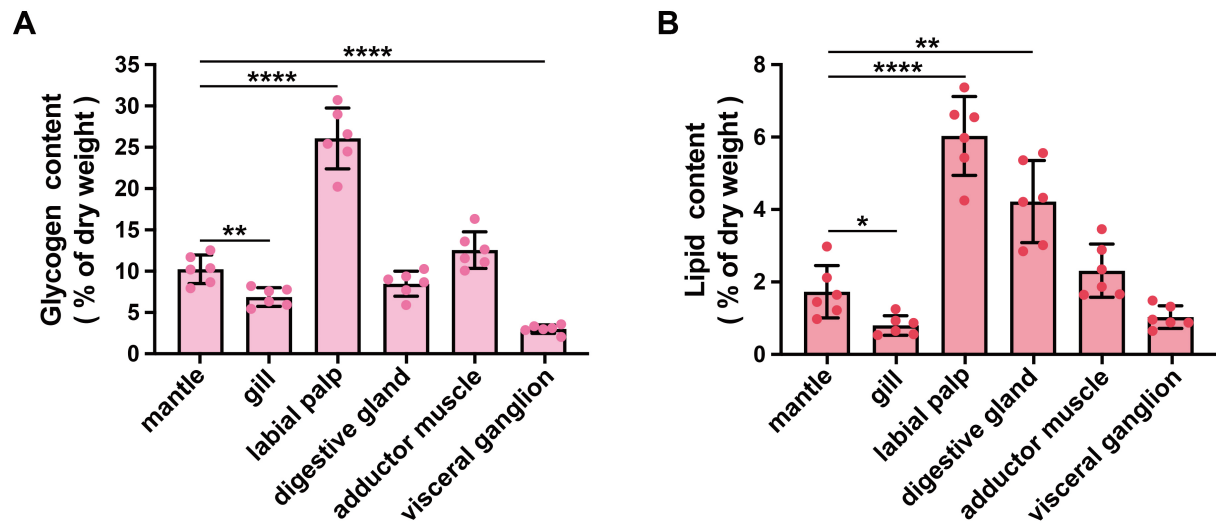


Fig. S2. Glycogen and lipid content in the mantle, gill, labial palp, digestive gland, adductor muscle and visceral ganglion. $n = 6$. Data are represented as mean \pm SD in (A, B), where statistical significance was calculated using one-way ANOVA. $*p < 0.05$, $**p < 0.01$, $****p < 0.0001$.

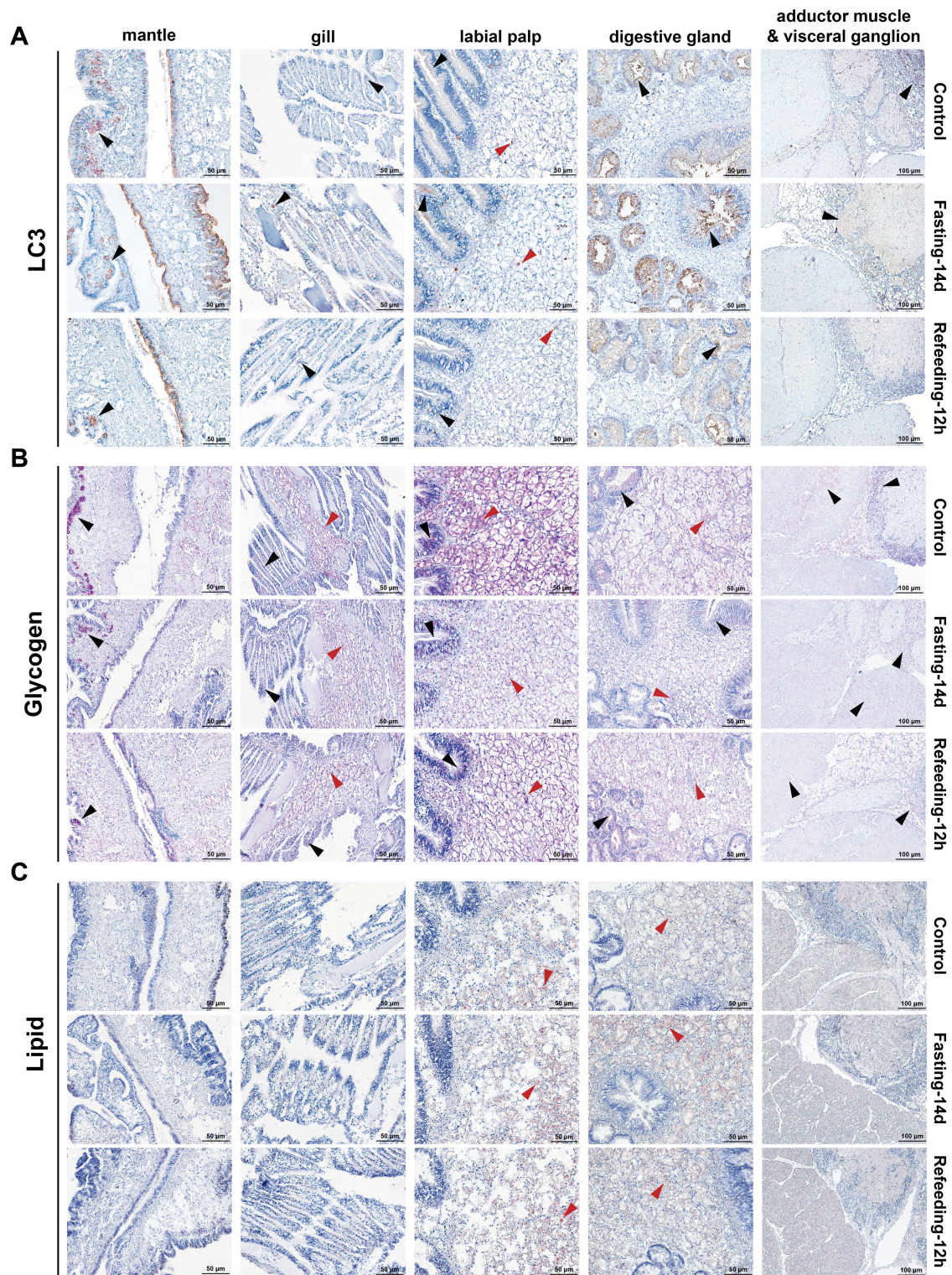


Fig. S3. Signals for the autophagy marker (A) LC3, (B) glycogen, (C) lipid in mantle, gill, labial palp, gonad, digestive gland, adductor muscle and visceral ganglion were observed after 14 d of fasting followed by 12 h of refeeding. Arrows indicate dense distribution of signals in the CE (black) and VCT (red) cells. Scale bars: 50 μm.

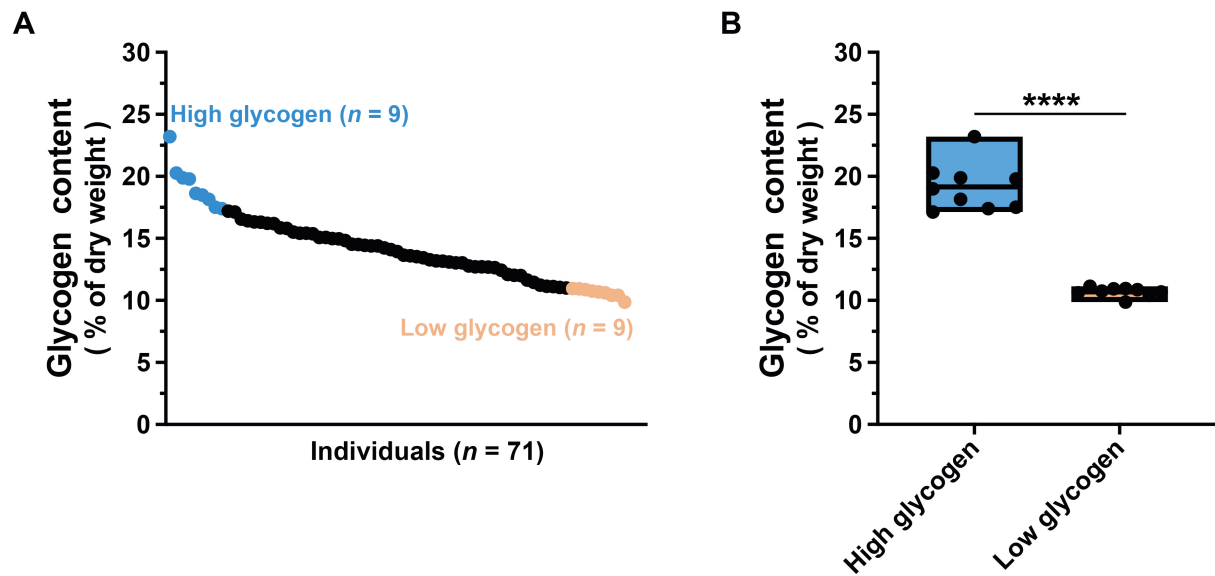


Fig. S4. Glycogen content in high glycogen and low glycogen groups. **A** Glycogen content in the labial palp dissected from 71 oyster individuals. Blue and pink points represent oyster samples with high and low glycogen, respectively. **B** The highest (average 19.15%) and lowest (average 10.7%) glycogen contents of 9 individuals sampled from 71 individuals, defining the high and low glycogen groups, respectively. Data are represented as mean \pm SD in **(B)**, where statistical significance was calculated using Student's *t* test. **** $p < 0.0001$.

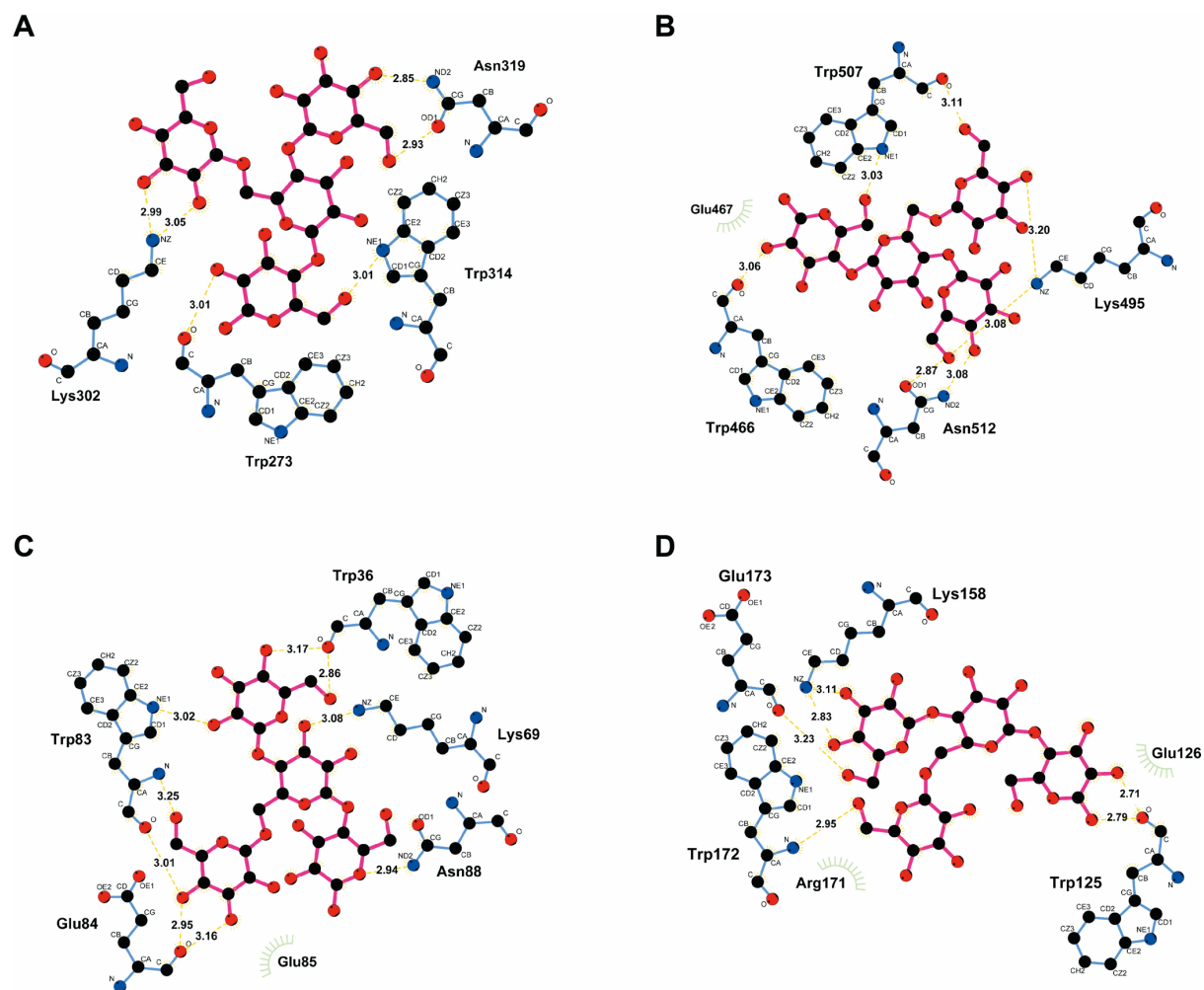


Fig. S5. Two dimensional views of docking models of glycogen with STBD1 from (A) mouse, (B) zebrafish, (C) *C. gigas*, and (D) a *C. gigas* STBD1 *in silico* mutant with CBM20 moved to the C-terminus. Hydrophobic residues are indicated by green radiations.

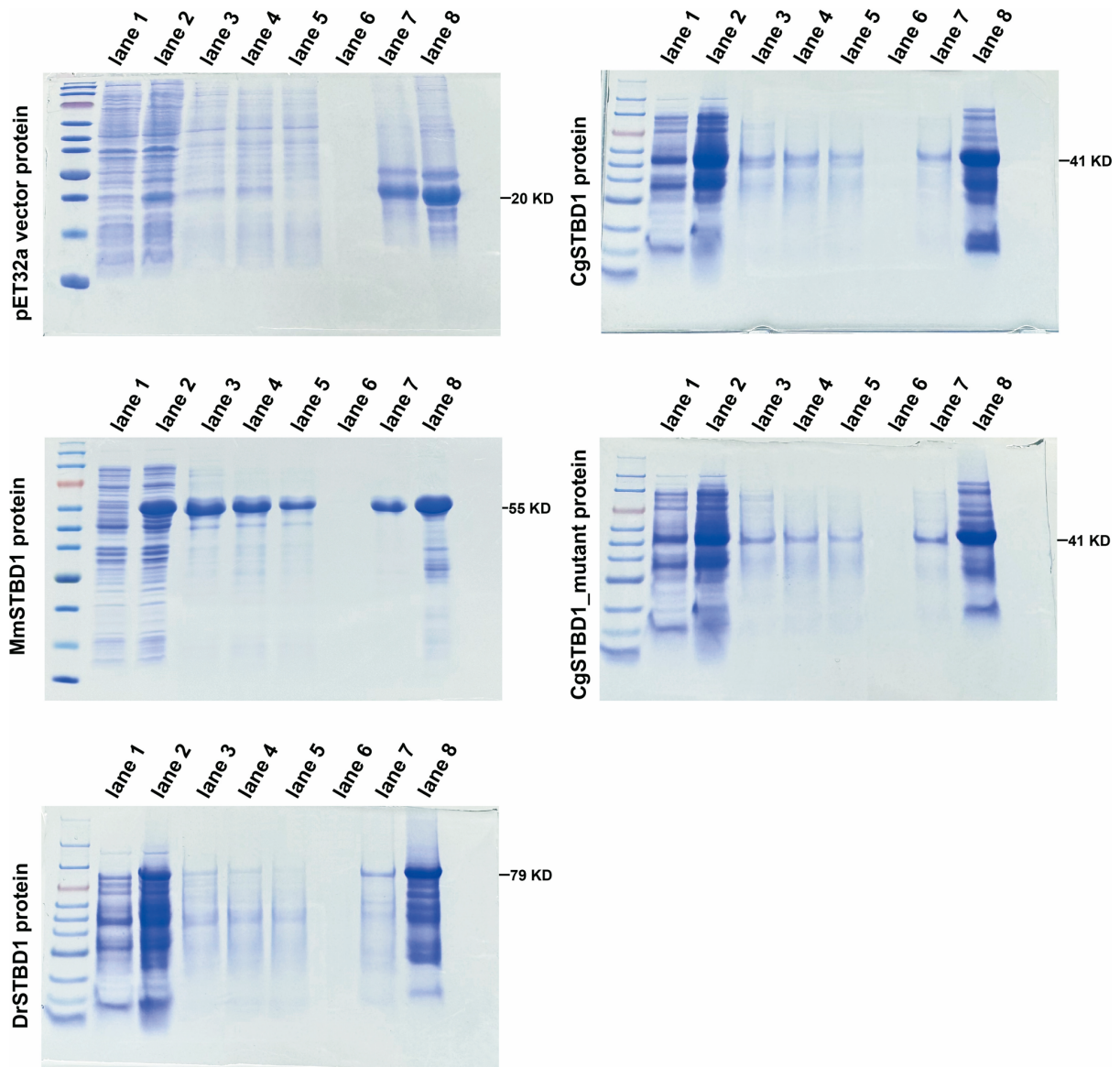
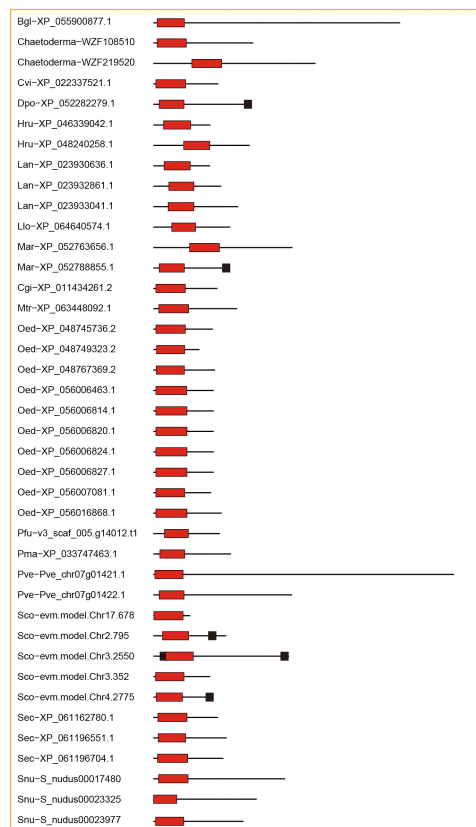
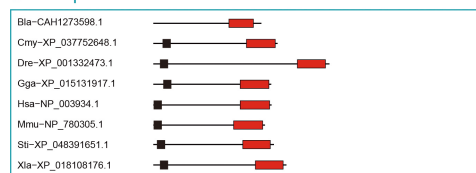


Fig. S6. SDS-PAGE was used to verify the molecular weights of pET32a vector recombinant proteins for STBD1 from mouse, zebrafish, wide-type *C. gigas* and a mutant *C. gigas* STBD1 with CBM20 moved to the C-terminus. Lane 1: prior to induction; lane 2: post induction; lane 3: bacterial lysate; lane 4: post-lysis supernatant; lane 5: flow-through fraction; lane 6: washing buffer; lane 7: elution buffer; lane 8: concentration buffer. Abbreviations used: Mm, *Mus musculus*; Dr, *Danio rerio*; Cg, *Crassostrea gigas*.

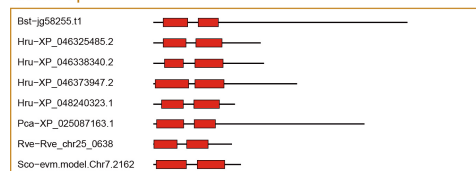
STBD1α



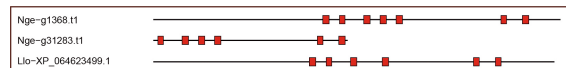
STBD1β



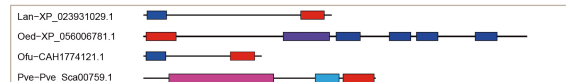
STBD1γ



STBD1δ



STBD1-related



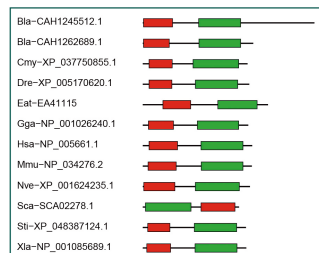
Domains (InterPro entrie):

- TM helix (identified with TMHMM2.0)
- Carbohydrate binding module family 20 (IPR002044)
- Glycerophosphodiester phosphodiesterase domain (IPR030395)
- Dual specificity phosphatase, catalytic domain (IPR003340)
- Ankyrin repeat (IPR002110)
- SOCS box domain (IPR01496)
- EF-hand domain (IPR002048)
- Peptidase M12B, ADAM/repolysin (IPR001590)
- Glycosyl hydrolase, family 13, catalytic domain (IPR006047)
- IPT domain (IPR002909)

Length of amino acid sequence:

Nge-g1368.11, Nge-g31283.11, Lio-XP_064623499.1: — 100 aa
Other proteins: — 100 aa

LAF



GPCPD1

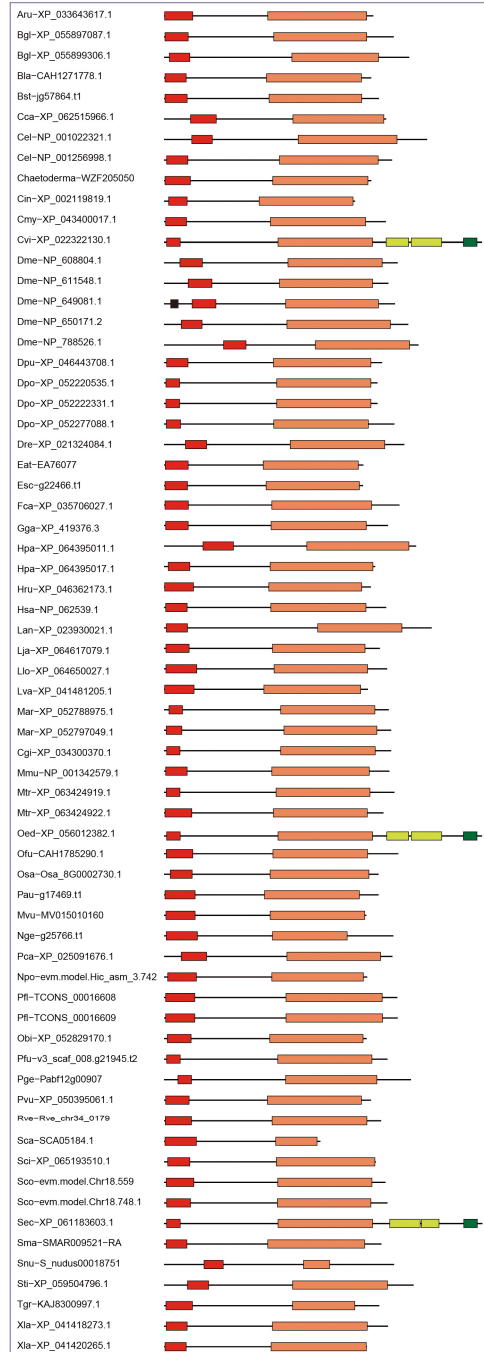


Fig. S7. Domain arrangements of CBM20 containing proteins. The proteins containing

CBM20 domain(s) were classified into seven types based on domain architectures. Briefly, among all identified proteins, those with CBM20 and dual specificity phosphatase domains were considered as LAF; those with CBM20 and glycerophosphodiester phosphodiesterase domains as GPCPD1; those with a single N-terminal CBM20 domain as STBD1 α ; those with one C-terminal CBM20 domain as STBD1 β ; those with two N-terminal CBM20 domains as STBD1 γ ; those with more than two N-terminal CBM20 domains as STBD1 δ ; and those with other domains such as EF-hand, peptidase M12B, IPT or glycosyl hydrolase family 13 as STBD1-related proteins. The corresponding abbreviations of species names are shown in Supplementary Table S1.

Supplemental references

1. Acheson, K. J., Flatt, J. P. & Jéquier, E. Glycogen synthesis versus lipogenesis after a 500 gram carbohydrate meal in man. *Metab.* **31**, 1234-1240 (1983).
2. Hewitt, M., Going, S., Williams, D. & Lohman, T. Hydration of the fat-free body mass in children and adults: implications for body composition assessment. *Am J Physiol.* **265**, E88-E95 (1993).
3. Wang, Z. et al. Total body protein: A new cellular level mass and distribution prediction model. *Am J Clin Nutr.* **78**, 979-984 (2003).
4. Javaid, S., Javid, A., Farooq, U., Kiran, U. & Akmal, T. Variations in meat chemical composition of some captive avian species. *J Pure Appl Agric.* **2**, 57-65 (2017).
5. Gang, X. & Juan, N. Effects of partial and complete food deprivation on compensatory growth of juvenile soft-shelled turtle (*Pelodiscus sinensis*): temporal

- patterns in growth rate and changes in body composition. *Acta Hydrobiol Sin.* **31**, 214-219 (2007).
6. Brenes Soto, A., Dierenfeld, E., Bosch, G., Hendriks, W. & Janssens, G. Gaining insights in the nutritional metabolism of amphibians: analyzing body nutrient profiles of the African clawed frog, *Xenopus laevis*. *PeerJ.* **7**, e7365 (2019).
 7. Arunagiri, T., Pandian, A. & Ramesh, S. Biochemical Composition in Edible Tissues of *Epinephelus malabaricus* (Bloch and Schneider, 1801) from Nagapattinam Coast, Tamil Nadu, India. *Int J Sci Res Biol Sci.* **6**, 125-127 (2019).
 8. Jiang, S. et al. Comparison of biochemical composition of commercial sea cucumbers, *Apostichopus japonicus* and *Parastichopus californicus*, under the same culture conditions. *J Sci Food Agric.* **102**, 5452-5459 (2022).
 9. Ohtsu, T., Kimura, M. T. & Hori, S. H. Energy storage during reproductive diapause in the *Drosophila melanogaster* species group. *J Comp Physiol B.* **162**, 203-208 (1992).
 10. Church, R. B. & Robertson, F. W. A biochemical study of the growth of *Drosophila melanogaster*. *J Exp Zool.* **162**, 337-351 (1966).
 11. Zečić, A., Dhondt, I. & Braeckman, B. The nutritional requirements of *Caenorhabditis elegans*. *Genes Nutr.* **14**, 15 (2019).
 12. Liu, S., Li, L., Wang, W., Busu, L. & Zhang, G. Characterization, fluctuation and tissue differences in nutrient content in the Pacific oyster (*Crassostrea gigas*) in Qingdao, northern China. *Aquac Res.* **51**, 1353-1364 (2020).